A Unified Analogy-Based Computation Methodology From Elasticity to Electromagnetic-Chemical-Thermal Fields and a Concept of Multifield Sensing

Xin Zhang[1]
School of Mechanical and Electrical Engineering,
University of Electronic Science and
Technology of China,
Chengdu 611731, China;
Department of Mechanical Engineering,
Northwestern University,
Evanston, IL 60208
e-mail: zhangxin@uestc.edu.cn

Q. Jane Wang[1]
Department of Mechanical Engineering,
Northwestern University,
Evanston, IL 60208
e-mail: qwang@northwestern.edu

This paper reports a unified analogy-based computation methodology, together with a concept of multifield, multifunctional sensing, from elasticity to electromagnetic-chemical--thermal fields, via utilizing the similarities of mechanical-electromagnetic-chemical-thermal (MEMCT) field variables, governing equations, and the material properties pertaining to each individual field. Two equivalences are systemized, which are the field-formulation equivalence and surface-value equivalence. Due to similarity, a number of thermal, electromagnetic, or chemical solutions can be obtained from the direct degeneration of existing mechanical solutions by making specified equivalences of $2G \leftrightarrow k_0 \leftrightarrow \varpi_0 \leftrightarrow \mu_0 \leftrightarrow \beta_0$ *with* G *for shear modulus,* k_0 *for heat conductivity,* ϖ_0 *for dielectric permittivity,* μ_0 *for magnetic permeability, and* β_0 *for chemical diffusivity, as well as by setting Poisson's ratio* $\nu \to 0.5$*. These specified equivalences enable quick solutions to other fields directly from mechanics formulations, such as those in the forms of the Galerkin vectors and Papkovich-Neuber potentials, and field coupling, by means of analogy. Several examples are given, one is used to demonstrate that the field solutions of a layered half-space with imperfect thermal, electromagnetic, or chemical interfaces can be readily obtained from the elastic solutions involving interfacial imperfections via the obtained formulation equivalence. A set of simple equations are derived to relate surface behaviors of different fields via the obtained surface-value equivalence, on which a concept of multifield sensing is proposed.* [DOI: 10.1115/1.4053910]

Keywords: similarity, equivalence, mechanics, electromagnetics, diffusion, heat conduction, contact, contact area, contact mechanics, multiphysics modeling and simulation, tribological systems, tribology

1 Introduction

In nature, the macroscopic energy of a material system is commonly in the form of mechanical, thermal, electromagnetic, and chemical (MEMCT) energies [1–4]. Therefore, many research efforts have mainly been focused on basic issues of individual mechanical, thermal, electromagnetic, or chemical fields. It is well known that these fields have certain similarities, and recently, problems of interdisciplinary and multifield features have drawn increasingly strong attention.

In many cases of technology developments, the mechanical effects, such as power transmission and contact of various material systems [5,6], have been studied in great detail, for example, indentation mechanics of layered [7–9] and functionally graded [10,11] materials using analytical or numerical methods, micromechanics of materials involving inhomogeneities or inclusions [12–15] by the phase-field model or the equivalent inclusion method, and nanomechanics of thin films and nano/microstructures [16–21] by the theories of strain-gradient plasticity or couple-stress elasticity. In heat transfer, a great deal of work has been focused on capturing the thermal behaviors of different material systems, among them are the development of the theories of heat transfer [22] and the studies of heat conduction in layered [23–25] and functionally graded [26,27] materials, as well as in materials involving inhomogeneities or inclusions [28–30]. Likewise, the Maxwell equations describe how the electric and magnetic fields are generated and mutually influenced [31,32]. On the interaction of materials, researchers have developed a mathematical framework to describe the mixture behaviors of material systems with diffusion, known as the mixture theory [33–37].

Similarities in some aspects of mechanical, thermal, electromagnetic, and chemical fields have been identified, and related quantities have been widely used for dimension analyses in surface/interfacial mechanics and structural mechanics [37–40]. Actually, the concept analogy across mechanical field, thermal, and electric/magnetic fields can be dated back to how the related theories were developed, from Einstein who imagined a "flow" of electric charge or heat in analogy to a mechanical force [41], from Fourier's law for heat conduction and Ohm's law for electricity, which were primarily inspired by Newton's law of cooling, especially from Thompson [42], who derived the concepts of different physical fields from their mathematical analogy. The thought of analogy, for example, between heat flow and mass diffusion, has to enable the use of the solution methods for thermal or thermomechanical systems to analyze diffusion, poroelastic, or chemo-mechanical problems, among them are the numerical manifold method for transient moisture diffusion in graded materials [43] in analogy to the corresponding transient thermal analysis [26], the equivalent inclusion method for frictional heating in inhomogeneous half-spaces [29] in analogy to the corresponding inclusion problem in elasticity [44], the unified solution approach for poroelasticity and thermoelasticity [45,46], the prediction method for the conversion between a thermal-energy flow and a mass transport [47], the

[1]Corresponding authors.

Manuscript received November 20, 2021; final manuscript received February 18, 2022; published online March 4, 2022. Assoc. Editor: Joichi Sugimura.

analogy between the shear stress in a twisted bar and a stretched soap film [48], and the analogy on material properties among electric, elastic, and piezoelectric parameters [49]. These investigations have intensively explored different facets of the MEMCT fields by analogies of their characters, but still involve resolving and re-deriving the field equations of the material systems under consideration.

Long-time mechanics research has resulted in rich theories and solutions for wide ranges of material structures and systems (e.g., layered materials, functionally graded materials, composite materials). This work proposes a novel methodology for multi-theory analogy across the MEMCT fields for a wide range of material systems including full-space, half-space, and layered materials, with or without eigenstrains, loaded by surface or internal sources. The methodology and solution framework are based on the conceptual analogy and mathematical similarities of a number of MEMCT field variables, governing equations, and their own material properties, which can help to utilize existing mechanics results to solve other complicated problems. The proposed MEMCT analogy methodology also expands the electromagnetic-elastic analogy theory [50,51] and enriches our previous MEMCT coupling theory [2] for in-depth understanding of multifield interactions and conversions. Further, it is expected that the systematic theoretical analogy and field equivalence may stimulate certain technological inventions or engineering method integration.

In this paper, analogy is the methodology to view the similarity between physical terms in mathematical expressions, and equivalence means quantification with the same expression.

2 MEMCT Analogy From the Mechanical Point of View

Figure 1 presents the main variables and governing equations for mechanical, thermal, electromagnetic, and chemical fields.

In the mechanical field, the gradient of the displacement vector u_i leads to the elastic strain tensor $\varepsilon_{ij}=(u_{i,j}+u_{j,i})/2$. The elastic strain tensor, ε_{ij}, and elastic stress tensor, σ_{ij}, are linked by the constitutive laws of $\sigma_{ij}=c_{ijkl}\varepsilon_{kl}$, with c_{ijkl} for the elastic property tensor. The elastic stress tensor, σ_{ij}, should satisfy the mechanical equilibrium of $\sigma_{ij,i}+f_i=\rho\partial^2 u_i/\partial t^2$, where f_i is the body force component, ρ is the mass density, and t is the time.

In the thermal field, the gradient of temperature rise T is defined as the vector θ_i satisfying the equation of $\theta_i=-T_{,i}$. The Fourier's law for heat conduction defines heat flux q_i as $q_i=k_{ij}\theta_j$, with k_{ij} for the heat conductivity tensor. The first law of thermodynamics is written in the form of $-q_{i,i}+q_0=\rho C_p\partial T/\partial t$, where q_0 is the strength of a volumetric heat source, C_p is the specific heat capacity.

In the electromagnetic field, the gradient of electric potential φ is the strength of the electric field, expressed as $E_i=-\varphi_{,i}$, while the gradient of magnetic potential ϕ is the strength of the magnetic field with $H_i=-\phi_{,i}$. The constitutive relationships for electricity without polarization is $D_i=\varpi_{ij}E_j$, while for magnetism without magnetization is $B_i=\mu_{ij}H_j$, where ϖ_{ij} is the dielectric permittivity tensor, μ_{ij} is the magnetic permeability tensor, D_i is the electric displacement vector, and B_i is the magnetic induction vector. The electric displacement should satisfy Gauss' law for electric field of $-D_{i,i}+\rho_f=0$, with ρ_f for free charge density, and the magnetic induction should satisfy Gauss' law for magnetism of $B_{i,i}=0$. Furthermore, the Maxwell-Faraday equation $\nabla\times\mathbf{E}=-\partial\mathbf{B}/\partial t$ and Ampère's circuital law $\nabla\times\mathbf{H}=\partial\mathbf{D}/\partial t+\mathbf{J}_f$ (with $\mathbf{J}_f$ for current density) govern the variation of the electromagnetic field.

In the chemical field, the gradient of mass concentration N is defined as the vector ϑ_i, satisfying $\vartheta_i=-N_{,i}$. The diffusion flux vector, ξ_i, can be given by Fick's first law of $\xi_i=\beta_{ij}\vartheta_j$, with β_{ij} for the diffusivity tensor. The mass balance in a diffusion process is $-\xi_{i,i}+W_0=\rho\frac{\partial N}{\partial t}$, where W_0 is the intensity of a local mass

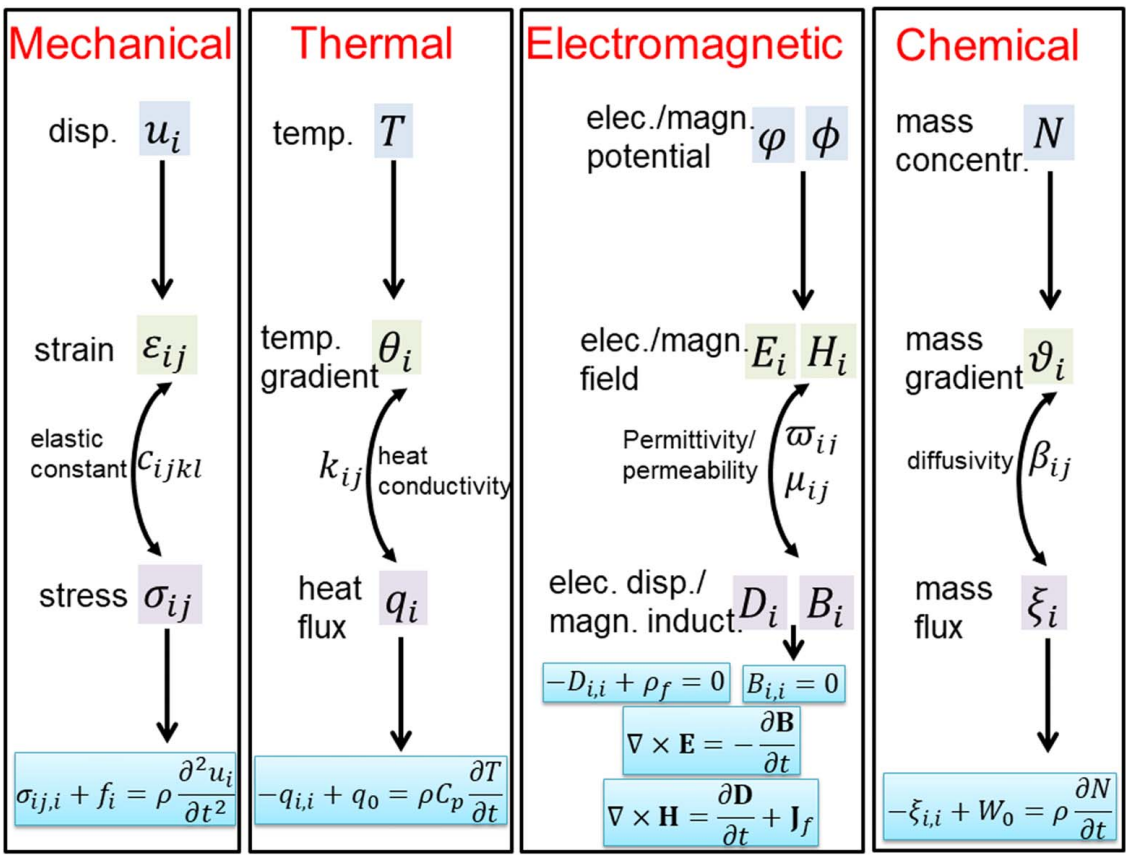

Fig. 1 Major variables and governing equations in the mechanical, thermal, electromagnetic, and chemical fields, where the double-end arced arrows mean field relationships

source, such as the rate of a chemical reaction. Here, a linear process is assumed; however, a nonlinear diffusion law can also be implemented if a localized linearization is possible.

2.1 Similarities. Defining a generalized field collection Φ, satisfying $\Phi = (u_i \leftrightarrow T \leftrightarrow \varphi \leftrightarrow \phi \leftrightarrow N)$, a generalized dual variable collection Ψ, satisfying $\Psi = (\sigma_{ij} \leftrightarrow -q_i \leftrightarrow -D_i \leftrightarrow -B_i \leftrightarrow -\xi_i)$, and a generalized material property C_M, yielding $C_M = (c_{ijkl} \leftrightarrow k_{ij} \leftrightarrow \varpi_{ij} \leftrightarrow \mu_{ij} \leftrightarrow \beta_{ij})$, with "$\leftrightarrow$" for equivalence, results in the generalized constitutive law of $\Psi = C_M \cdot \Phi_{,i}$. If the time-related terms of the MEMCT fields are defined by a function, $\Omega(\Phi, t)$, with respect to time t and field collection Φ, the generalized equilibrium equation can be written as $\Psi_i + F_i = \Omega(\Phi, t)$, where $F_i = (f_i \leftrightarrow q_0 \leftrightarrow \rho_f \leftrightarrow 0 \leftrightarrow W_0)$ is the strength of a generalized volumetric source.

2.2 Differences. The above variables can make a complete analogy, but this analogy should not be stretched too far.

The variables in elasticity have higher orders than those in other fields. For the field collection of $\Phi = (u_i \leftrightarrow T \leftrightarrow \varphi \leftrightarrow \phi \leftrightarrow N)$, elastic displacement u_i is a first-order tensor (or vector), while temperature rise T, electric potential φ, magnetic potential ϕ, and mass concentration N are zero-order tensors (or scalars). For the material properties of $C_M = (c_{ijkl} \leftrightarrow k_{ij} \leftrightarrow \varpi_{ij} \leftrightarrow \mu_{ij} \leftrightarrow \beta_{ij})$, elastic constant c_{ijkl} is a fourth-order tensor, while heat conductivity k_{ij}, dielectric permittivity ϖ_{ij}, magnetic permeability μ_{ij}, and chemical diffusivity β_{ij} are second-order tensors. In the dual variable collection of $\Psi = (\sigma_{ij} \leftrightarrow -q_i \leftrightarrow -D_i \leftrightarrow -B_i \leftrightarrow -\xi_i)$, elastic stress σ_{ij} is a second-order tensor, while heat flux q_i, electric displacement D_i, magnetic induction B_i, and diffusion flux ξ_i are vectors.

The time scales in the MEMCT fields are different. In elasticity, the time-related term is $\Omega = \rho \partial^2 u_i / \partial t^2$, while it is $\Omega = \rho C_p \partial T / \partial t$ in the thermal field, and $\Omega = \rho \partial N / \partial t$ in the chemical field. However, the dependence of the electromagnetic field on time is governed by Maxwell's equations, i.e., the sum of Gauss' laws for electric field and magnetism, the Maxwell-Faraday equation, and Ampère's circuital law.

For clarity, the similarities and differences of the MEMCT field variables, governing equations, and the material properties pertaining to each individual field, are described in Fig. 1, which shows that the variables in the mechanical field have higher orders than those in the other fields. Theoretically, the lower-order variables can be obtained from the degradation of the corresponding higher-order mechanical variables. According to Thomson and Wise's ideas [42,52], the vision from the mechanical field should foresee a reasonable path to describe the analogy.

2.3 Mechanical-Thermal Analogy. Consider a homogeneous and isotropic half-space $\mathcal{B}$, subjected to a time-varied normal force, $\bar{p}(x, y, t)$, on its boundary along the z direction, which is set as the direction of the surface normal, shear transtions, $\bar{s}_1(x, y, t)$ and $\bar{s}_2(x, y, t)$ along the x and y directions or a time-varied heat flux, $\bar{q}(x, y, t)$, normal to the surface. For any material point (x, y, z) inside $\mathcal{B}$, the initial condition at time $t = 0$ is

$$\begin{aligned} u_x(x, y, z, 0) &= u_x^0(x, y, z) \\ u_y(x, y, z, 0) &= u_y^0(x, y, z) \\ u_z(x, y, z, 0) &= u_z^0(x, y, z) \end{aligned} \tag{1}$$

for elasticity, and

$$T(x, y, z, 0) = T^0(x, y, z) \tag{2}$$

for temperature, where u_i^0 is the initial displacement, T^0 is the initial temperature. For time $t > 0$, the boundary condition is

$$\begin{aligned} \sigma_{zx}(x, y, 0, t) &= \bar{s}_1(x, y, t) \\ \sigma_{zy}(x, y, 0, t) &= \bar{s}_2(x, y, t) \\ \sigma_{zz}(x, y, 0, t) &= -\bar{p}(x, y, t) \end{aligned} \tag{3}$$

for elasticity, and

$$k_0 \frac{\partial T(x, y, 0, t)}{\partial z} = -\bar{q}(x, y, t) \tag{4}$$

for heat conduction, where $\sigma_{ij} = \sigma_{ji}$ is the stress component, k_0 is an isotropic heat conductivity.

By comparing Eqs. (1) with (2), and Eqs. (3) with (4), and considering that shear tractions have no influence in system degeneration, to be set to zero, there is a complete analogy between the variables in elasticity and those in heat conduction:

$$\text{displacement } u_z \;\leftrightarrow\; \text{temperature } T \tag{5}$$

$$\text{pressure } \bar{p} \;\leftrightarrow\; \text{surface heat flux } \bar{q} \tag{6}$$

$$\text{stress } \sigma_{zz} \;\leftrightarrow k_0 \frac{\partial T}{\partial z} \tag{7}$$

where stress σ_{zz} can be written as

$$\sigma_{zz} = \lambda \Theta + 2G u_{z,z} \tag{8}$$

with $\lambda = \dfrac{\nu E}{[(1+\nu)(1-2\nu)]}$ and $G = \dfrac{E}{[2(1+\nu)]}$ for the Lamé constants, E for Young's modulus, ν for Poisson's ratio, $\Theta = u_{x,x} + u_{y,y} + u_{z,z}$ for the volumetric strain. In view of Eqs. (7) and (8), complete equivalences of $u_z \leftrightarrow T$ and $\sigma_{zz} \leftrightarrow k_0 \partial T / \partial z$ lead to (i) the volumetric strain $\Theta = 0$, which is corresponding to incompressible elasticity with Poisson's ratio $\nu \to 0.5$; and (ii) $2G \leftrightarrow k_0$. Such equivalences are partly based on the pioneer works reported in Refs. [29,53–56].

Furthermore, in order to compare the transient behaviors in elasticity and heat conduction, one of the Lamé-Navier equations is

$$(\lambda + \mu)\Theta_{,z} + G\nabla^2 u_z + f_z = \rho \frac{\partial^2 u_z}{\partial t^2} \tag{9}$$

and the heat-conduction equation is

$$k_0 \nabla^2 T + q_0 = \rho C_p \frac{\partial T}{\partial t} \tag{10}$$

where f_z is the body force along the z-direction. Again, there is a complete equivalence between body force and volumetric heat source: $f_z \leftrightarrow q_0$.

The complete equivalence of Eqs. (9) and (10) is resulted from (i) $\Theta_{,z} = 0$; (ii) $\dfrac{\rho}{G}\dfrac{\partial^2 u_z}{\partial t^2} \leftrightarrow \dfrac{\rho C_p}{k_0}\dfrac{\partial T}{\partial t}$. For (i) $\Theta_{,z} = 0$, this is naturally satisfied due to $\Theta = 0$ stated below Eq. (8). Moreover, if z, or the power of z, is a multiplier of a term in an elastic solution, for examples, $zf(x,y,z)$, $z^2 f(x,y,z)$, variable z should be set zero, and likewise for x or y removal if the excitation source is along the x or y direction. For (ii), it is found that the time scales in elasticity and in heat conduction are different. If elastic displacement u_z is defined as a harmonic function F_e with elastic wave frequency ω_e, and temperature T is defined as another harmonic function F_t with thermal wave frequency ω_t, condition $\dfrac{\rho}{G}\dfrac{\partial^2 u_z}{\partial t^2} \leftrightarrow \dfrac{\rho C_p}{k_0}\dfrac{\partial T}{\partial t}$ yields $\omega_e^2 \leftrightarrow -\dfrac{\mathrm{i}C_p}{2}\omega_t$. For example, if an elastic displacement has a harmonic solution of $u_z(x, y, z, t) = Z_1(x, y, z) \cdot e^{-\mathrm{i}\omega t}$ with ω for the wave frequency, temperature should have a harmonic solution in the form of $T(x, y, z, t) = Z_2(x, y, z) \cdot e^{\frac{2\omega^2}{C_p} t}$.

In summary, such a complete equivalence between elasticity and heat conduction is obtained by setting: (i) Poisson's ratio $\nu \to 0.5$;

(ii) shear modulus $2G \leftrightarrow$ heat conductivity k_0; (iii) removing terms multiplied by z^n in the elastic solutions, such as zu_z, z^2u_z, $z^nf(x,y,z)$, etc.; and (iv) elastic wave frequency $\omega_e^2 \leftrightarrow$ thermal wave frequency $-iC_p/2\omega_t$. Two examples (the Papkovich-Neuber potentials and Galerkin vectors) are given below to explain how to make use of the equivalent method between elasticity and heat conduction.

2.3.1 *Solutions Using Papkovich-Neuber Potentials*

(1) Half-space

Considering an isotropic and homogeneous elastic half-space, whose surface is subjected to the normal force P at the origin and along the z-direction, the elastic displacement, u_z, can be found in Ref. [6]

$$u_z(x, y, z) = \frac{P}{4\pi G}\left[\frac{z^2}{r^3} + \frac{2(1-\nu)}{r}\right] \tag{11}$$

where $r = \sqrt{x^2 + y^2 + z^2}$.

For the problem of an isotropic and homogeneous half-space subjected to a surface point heat source, Q, by making $\nu = 0.5$, $2G \to k_0$, $P \to Q$, and removing the term multiplied by z^n, which means to remove the first term, z^2/r^3, in Eq. (11), the temperature distribution can be obtained from Eq. (11)

$$T(x, y, z) = \frac{Q}{2\pi k_0}\frac{1}{r} \tag{12}$$

which is identical to that in Ref. [57].

(2) Layered half-space

Because it is difficult to obtain the space-domain analytical solutions for a layered half-space subjected to a unit normal force, the frequency response functions (FRFs) are usually solved first. The FRFs for normal displacement u_z can be found in Ref. [58], which are

$$\begin{aligned}\overset{\approx}{F}_r^{(u_z)} = &\frac{1}{2G_r}[-\alpha(D_r e^{-\alpha z_r} - \bar{D}_r e^{\alpha z_r}) - (3-4\nu_r)(C_r e^{-\alpha z_r} + \bar{C}_r e^{\alpha z_r}) \\ &- z_r\alpha(C_r e^{-\alpha z_r} - \bar{C}_r e^{\alpha z_r})]\end{aligned} \tag{13}$$

where $\alpha = \sqrt{m^2 + n^2}$ denotes the distance of a node, (m, n), to the origin of the frequency domain. Subscript $r = 1$ or 2 is used to distinguish variables associated with the layer or the substrate half-space, respectively. Coefficients C_r, $\bar{C}_r$, D_r and $\bar{D}_r$ ($\bar{C}_2 = \bar{D}_2 = 0$) can be found in Eqs. (22*a*)–(22*f*) of Ref. [58].

For the problem of a layered half-space subjected to a unit point heat source, by making $2G_r \leftrightarrow k_r$, $\nu_r = 0.5$, and removing the term with z and h multiplication, because h resembles z, which means to remove the last term, $z_r\alpha(C_r e^{-\alpha z_r} - \bar{C}_r e^{\alpha z_r})$, in Eq. (13), and the term multiplied by $2\alpha h$ in C_r, $\bar{C}_r$, D_r and $\bar{D}_r$. Therefore, the FRFs for temperature T can be obtained from Eq. (13)

$$\overset{\approx}{F}_r^{(T)} = \frac{1}{k_r}(C_r e^{-\alpha z_r} + \bar{C}_r e^{\alpha z_r}), \quad r = 1, 2 \tag{14}$$

where

$$C_1 = \frac{1}{\alpha(1 - k_3 e^{-2\alpha h})}$$

$$\bar{C}_1 = \frac{k_3 e^{-2\alpha h}}{\alpha(1 - k_3 e^{-2\alpha h})}$$

$$C_2 = \frac{(1 - k_3)e^{-\alpha h}}{\alpha(1 - k_3 e^{-2\alpha h})}$$

$$\bar{C}_2 = D_r = \bar{D}_r = 0$$

with h for layer thickness, and $k_3 = (k_1 - k_2)/(k_1 + k_2)$. Equations in (14) are identical to the FRFs for temperature in Ref. [25].

To be clear, Fig. 2 compares the surface temperature and subsurface heat flux distributions of a layered half-space solved by the current equivalence approach *via* the elastic solutions in Ref. [58] and the heat conduction solutions given in Ref. [25], using the discrete convolution-fast Fourier transform (DC-FFT) algorithm [59] with a $256 \times 256 \times 100$ grid on a physical domain of 6.0 mm × 6.0 mm × 4.0 mm, for the problem of a uniform surface heat input of density 2000 W/mm^2 on the region $\sqrt{x^2 + y^2} \le 1.0$ mm. The layer thickness is $h = 1.0$ mm, the substrate conductivity is $k_2 = 25$ W/mm·K, and the layer conductivity is $k_1 = 0.5k_2$ or $2.0k_2$. As shown in Figs. 2(*a*) and 2(*b*), respectively, the results of the temperature and heat flux from the current equivalence approach based on the elastic solutions in Ref. [58] are identical to those from the heat-conduction solutions given in Ref. [25].

2.3.2 *Solutions Built on the Galerkin Vectors.*

Consider an isotropic and homogeneous media (e.g., full-space or half-space) with or without a volumetric irregular region subject to eigenstrains distributed arbitrarily. The elastic displacement, u_i, caused by forces or eigenstrains, can be expressed in terms of the Galerkin vectors, F_i [60]

$$2Gu_i = 2(1 - \nu)F_{i,jj} - F_{j,ji} \tag{15}$$

Here and throughout this section, the standard index notation is used, where comma represents differentiation with respect to the suffix coordinate, and the Einstein summation convention is used for repeated index. Subscripts 1, 2, and 3 of variables indicate x, y, and z, respectively.

The Galerkin vector for elasticity has three components, but in most cases of heat conduction, only one of them is needed, which is the one for the z-direction to consider a half-space with its depth in z. The complete equivalence of $u_z \leftrightarrow T$ with the condition of Poisson's ratio $\nu \to 0.5$ leads to the temperature field in terms of the Galerkin vector for heat conduction, $F^T = F_i = F_3$, starting from Eq. (15)

$$2Gu_i = (F_{i,jj} - F_{j,ji})_{\nu \to 0.5} \to k_0 T = (F_{3,jj} - F_{3,33})_{\nu \to 0.5} = (F^T_{,jj} - F^T_{,33}) \tag{16}$$

Furthermore, substituting Eq. (16) into Eq. (9) results in $T = 1/k_0 D_1 F^T_{,jj}$, with D_1 for a constant, meaning that only one term of the F^T differentiation is sufficient. However, Eq. (15), or (16), is still used in the following to show the details of the equivalence approach.

It should be mentioned that, even though F^T is no longer a vector, it is still called the Galerkin vector for terminology consistence.

(1) Homogeneous full-space

Consider single unit mechanical forces at (x', y', z') in the x, y, or z directions of the full-space, the magnitudes of the Galerkin vectors are all the same as $F = \dfrac{R^I}{8\pi(1-\nu)}$, where $R^I = \sqrt{(x - x')^2 + (y - y'^2 + (z - z')^2}$. We can also define $R = \sqrt{(x - x')^2 + (y - y')^2 + (z + z')^2}$ for use later.

The z-direction elastic displacement at (x, y, z), u_z, given in Eq. (15), is the following, subjected to the equivalence treatment

$$\begin{aligned}2Gu_z = 2(1-\nu)F_{,jj} - F_{,33} = &\frac{1}{8\pi(1-\nu)} \\ &(4(1-\nu)\phi^I - \phi^I - (z - z')\phi^I_{,3}) \xrightarrow{\text{remove } z\text{-term}} \\ &\frac{3-4\nu}{8\pi(1-\nu)}\frac{1}{R^I}\end{aligned} \tag{17}$$

where $\varphi^I = 1/R^I$.

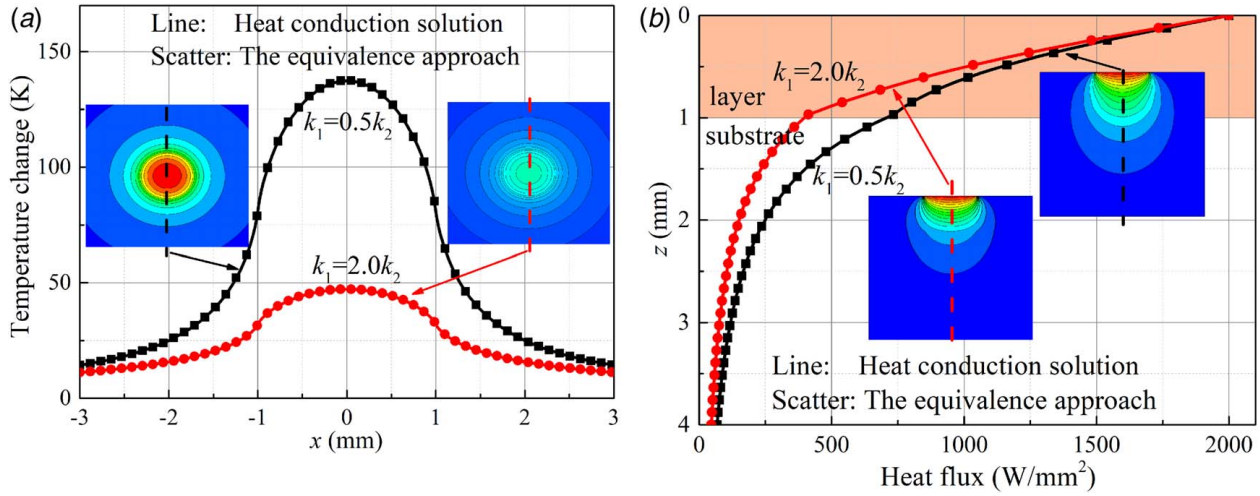

Fig. 2 (*a*) Surface temperature and (*b*) subsurface heat flux of a layered half-space solved by the current equivalence method and the heat-conduction solutions, for the problem of a uniform surface heat input of density 2000 W/mm^2 on the region $\sqrt{x^2+y^2} \le 1.0$ mm. The layer thickness is $h = 1.0$ mm, the substrate conductivity is $k_2 = 25$ W/mm·K, and the layer conductivity is $k_1 = 0.5k_2$ or $2.0k_2$.

By using the equivalence conditions between Eqs. (17) and (11), which are (i) Poisson's ratio $\nu \to 0.5$; (ii) shear modulus $2G \leftrightarrow$ heat conductivity k_0, which means setting $\frac{3-4\nu}{8\pi(1-\nu)(2G)} \to \frac{1}{4\pi(2G)} \sim \frac{1}{4\pi k_0}$ for a unit heat source, and (iii) removing the $z(z')$-multiplication term (done above in Eq. (17)) in the elastic solution, Eq. (17) becomes the following for heat flux Q

$$T(x, y, z) = \frac{1}{4\pi k_0}\frac{Q}{R^I} \tag{18}$$

where displacement $u_z \leftrightarrow$ temperature T. Equation (18) is exactly the full-space heat-conduction solution for the temperature field under a steady point source, one half that of the half-space solution [6], to be discussed below, under the same heat source. At the same time, the Galerkin vector for heat conduction in the full-space is $F^T = \frac{1}{4\pi}R^I$ in equivalence to $F = \frac{R^I}{8\pi(1-\nu)}$ with setting Poisson's ratio $\nu \to 0.5$.

(2) Half-space with surface sources

For a half-space loaded by a unit surface force at (x', y') along the z-direction, the Galerkin vector is [61]

$$\boldsymbol{F} = \frac{1}{8\pi(1-\nu)}\begin{bmatrix} 0 \\ 0 \\ R^I + (3-4\nu)R - 2z\cdot z'\phi - 4Dz'\psi - 4HD\theta \end{bmatrix}^T \tag{19}$$

where $D = 1-2\nu$, $\theta = R - z\ln[R+z]$, $\psi = \ln[R+z]$. By dropping the terms with D and $z(z')$- multiplication, making $\nu \to 0.5$ inside the brackets, and noting that $R = R^I$ when $z' = 0$, Eq. (19) becomes

$$\boldsymbol{F} = \frac{1}{4\pi(1-\nu)}\begin{bmatrix} 0 \\ 0 \\ R^I \end{bmatrix}^T \tag{20}$$

The Galerkin vector for heat conduction in the half-space subjected to a surface source is from the third one of Eq. (20), $F^T = \frac{1}{2\pi}R^I$, which is twice that of the full-space solution, and so is the temperature field, the same as Eq. (12).

(3) Half-space with internal sources

The Galerkin vector for a single unit force at (x', y', z') along the z-direction inside the half-space is

$$\boldsymbol{F} = \frac{1}{8\pi(1-\nu)}\begin{bmatrix} 0 \\ 0 \\ R^I + (3-4\nu)R - 2z\cdot z'\phi - 4Dz'\psi - 4HD\theta \end{bmatrix}^T \tag{21}$$

The "displacement," u_z, is the following after dropping the $z(z')$-multiplication terms and making $\nu \to 0.5$

$$2Gu_z = \frac{1}{4\pi}\left(\frac{1}{R^I} + \frac{1}{R}\right) \tag{22}$$

Therefore, the temperature due to heat flux Q is

$$T = \frac{Q}{k_0}(F^T_{,jj} - F^T_{,33}) = \frac{Q}{4\pi k_0}\left(\frac{1}{R^I} + \frac{1}{R}\right) \tag{23}$$

Equation (23) is equivalent to Eq. (22) by letting $2G \leftrightarrow k_0$, and the Galerkin vector for heat conduction in the half-space with internal sources is from the third component of Eq. (21)

$$F^T = \frac{1}{4\pi}(R^I + R) \tag{24}$$

(4) Full-space materials with eigenstrains

Considering an isotropic and homogeneous full-space with a volumetric irregular region subject to eigenstrains e_{ij} distributed at (x', y', z') arbitrarily, the full-space elastic eigenstrain solutions are given in Refs. [62,63], where the Galerkin vector is $\boldsymbol{F}(\boldsymbol{x}) = \frac{G}{4\pi(1-\nu)}\int_\Omega (2\nu e_{kk}\boldsymbol{g}_c - e_{jk}\boldsymbol{g}_{jk})d\boldsymbol{x}' = \int_\Omega \boldsymbol{f}dx'$. Corresponding to eigenstrains, eigen-temperature is expected for heat-conduction problems. Letting Poisson's ratio $\nu \to 0.5$, which also means $e_{kk} = 0$ in mechanics, the integral core of the Galerkin vector becomes

$$\boldsymbol{f} = -\frac{G}{2\pi}\begin{bmatrix} e_{1j}R^I_{,j} \\ e_{2j}R^I_{,j} \\ e_{3j}R^I_{,j} \end{bmatrix}^T \tag{25}$$

Taking the third component of Eq. (25), and noting that e_{3j} is the equivalence to eigen-temperature gradient ΔT_j^*, $2G \leftrightarrow k_0$, with k_0 as the thermal conductivity of the eigen-temperature region, the integral core of the Galerkin vector for heat conduction in the full-space subjected to an eigen-temperature gradient is

$$f^T = -\frac{k_0}{4\pi}\Delta T_j^* R_{,j}^I \tag{25'}$$

The result is identical to that in Ref. [64].

Using Eq. (16) and dropping the $z(z')$-related terms, the integral core of temperature can be expressed as

$$T = \frac{1}{k_0}(f_{,jj}^T - f_{,33}^T) \rightarrow -\frac{1}{4\pi}e_{3j}(R_{,jkk}^I - R_{,j33}^I) \rightarrow -\frac{1}{4\pi}\Delta T_j^* \phi_{,j}^I \tag{26}$$

It should be mentioned that for this problem of full symmetry, any of the vectors in Eq. (25), or all, can be utilized to obtain the Galerkin-vector equivalence. But Eq. (26) cannot be directly obtained from the elastic displacement results by setting $\nu \rightarrow 0.5$ and $2G \leftrightarrow k_0$ and by dropping the $z(z')$- multiplication terms.

(5) Half-space with eigenstrains

For a half-space with eigenstrains, the integral cores of the Galerkin vectors for elasticity [15,62] become the following via the equivalence approach

$$\boldsymbol{g}_{i1} = -\frac{G}{2\pi}\begin{bmatrix} \frac{\partial(R^I + R)}{\partial x'} & \frac{\partial(R^I + R)}{\partial y'} & \frac{\partial(R^I + R)}{\partial z'} \\ 0 & 0 & 0 \\ 0 & 0 & 2R_{,1} \end{bmatrix}^T \tag{27}$$

$$\boldsymbol{g}_{i2} = -\frac{G}{2\pi}\begin{bmatrix} 0 & 0 & 0 \\ \frac{\partial(R^I + R)}{\partial x'} & \frac{\partial(R^I + R)}{\partial y'} & \frac{\partial(R^I + R)}{\partial z'} \\ 0 & 0 & 2R_{,2} \end{bmatrix}^T \tag{28}$$

$$\boldsymbol{g}_{i3} = -\frac{G}{2\pi}\begin{bmatrix} 0 & 0 & 0 \\ 0 & 0 & 0 \\ \frac{\partial(R^I + R)}{\partial x'} & \frac{\partial(R^I + R)}{\partial y'} & \frac{\partial(R^I + R - 2z \cdot z'\phi)}{\partial z'} \end{bmatrix}^T \tag{29}$$

Therefore, after converting the differentiations to x, y, z

$$\boldsymbol{f} = -e_{jk}\boldsymbol{g}_{jk} = \frac{G}{2\pi}\begin{bmatrix} -e_{1j}(R^I + R)_{,j} + 2e_{13}R_{,3} \\ -e_{2j}(R^I + R)_{,j} + 2e_{23}R_{,3} \\ -e_{3j}(R_{,j}^I - R_{,j}) \end{bmatrix}^T \tag{30}$$

Note that $e_{ij} = e_{ji}$. Only the third component of the above should be used, due to half-space symmetry, as the core of the Galerkin vector, and again, e_{3j} is the equivalence to eigen-temperature gradient ΔT_j^*, $2G \leftrightarrow k_0$, with k_0 as the thermal conductivity of the inhomogeneity. The integral core of the Galerkin vector for heat conduction in the half-space with eigen-temperature gradient is

$$f^T = -\frac{k_0}{4\pi}\Delta T_j^*(R_{,j}^I - R_{,j}) \tag{30'}$$

Thus, the integral core of temperature, from Eq. (16), is

$$T = \frac{1}{k_0}(f_{,jj}^T - f_{,33}^T) \rightarrow -\frac{1}{4\pi}\Delta T_j^*(\phi_{,j}^I - \phi_{,j}) \tag{31}$$

Equation (31) is identical to the result in Ref. [64].

In summary, the mechanical-thermal equivalence can be established with the following considerations: (i) If the mechanical formulations are structured from the Papkovich-Neuber solutions, which only have harmonic potentials, the equivalence can be implemented directly at the final solutions, or at any step of the solution derivation; (ii) If the mechanics solutions are built on the Galerkin vectors, use F_3 only due to solution symmetry for half-space problems, but use any or all of F_i is optional for the full-space solutions; (iii) Because the Galerkin-vector solutions include biharmonic potentials, not all terms in elasticity are proper for heat-conduction solutions. For homogeneous materials, direct result equivalence is appropriate, but for eigen-temperature and inhomogeneity problems, the equivalence should be done at the Galerkin-vector stage (Table 1).

The Galerkin vectors for elastic and heat-conduction problems are summarized below, where $\psi = \ln[R + (z + z')]$; $\theta = R - (z + z')\psi$.

2.4 Thermal-Chemical Analogy. Again, consider a chemical species diffusing into a homogeneous and isotropic half-space $\mathcal{B}$ cross its surface, with a time-varied surface diffusive flux $\bar{\xi}(x, y, t)$. For any material point (x, y, z) inside $\mathcal{B}$, the initial condition for mass concentration of the diffusive species at time $t = 0$ is

$$N(x, y, z, 0) = N^0(x, y, z) \tag{32}$$

with N^0 for the initial mass concentration of the diffusive species. For time $t > 0$, the boundary condition is

$$\beta_0 \frac{\partial N(x, y, 0, t)}{\partial z} = -\bar{\xi}(x, y, t) \tag{33}$$

where β_0 is the diffusivity.

It has been shown in Fig. 1, the chemical variables are in a complete analogy with the heat-conduction variables, i.e.

$$\text{mass concentration } N \leftrightarrow \text{ temperature } T \tag{34}$$

$$\text{surface diffusive flux } \bar{\xi} \leftrightarrow \text{ surface heat flux } \bar{q} \tag{35}$$

$$\text{diffusivity } \beta_0 \leftrightarrow \text{ conductivity } k_0 \tag{36}$$

$$\text{mass source } W_0 \leftrightarrow \text{heat source } q_0 \tag{37}$$

$$\frac{\partial N}{\partial t} \leftrightarrow C_p \frac{\partial T}{\partial t} \tag{38}$$

It is found from Eq. (38) that the time scales in chemical and thermal fields are different, but they are proportional. If mass concentration N is defined as a harmonic function, F_N, of diffusion wave frequency ω_N, and temperature T is defined as F_t of thermal wave frequency ω_t, mentioned in Sec. 2.3, condition $\frac{\partial N}{\partial t} \leftrightarrow C_p \frac{\partial T}{\partial t}$ result in $\omega_N \leftrightarrow C_p \omega_t$. The equivalence between heat conduction and chemical diffusion also affects the equivalence between elasticity and chemical diffusion.

2.5 Thermal-Electromagnetic Analogy. The dependence of electromagnetic fields on time is governed by Maxwell's equations, which means that the magnetic and electric fields are mutually affected. The electromagnetic wave propagation can be equivalent to the elastic wave propagation, as stated in Ref. [51]. Considering the fact that the frequency of magnetoelectric waves is much higher than those of the mechanical, thermal, or chemical diffusion waves [66], only the static electromagnetic solutions are carried out here. If the transient behaviors of the electromagnetic field are ignored, the Maxwell-Faraday equation and Ampère's circuital law vanish, and only the Gauss' laws for electricity and magnetism remain.

Table 1 Elasticity-heat-conduction equivalence from elastic Galerkin-vector solutions

	Galerkin-vector, elastic field	Elastic displacements	Galerkin-vector, temperature field	Temperature	Comment
Full-space, point source	$F=\frac{R^I}{8\pi(1-\nu)}$ from Ref. [65]	Unit force $2Gu_z=\frac{1}{8\pi(1-\nu)}\begin{pmatrix}4(1-\nu)\phi^I-\phi^I\\-(z-z')\phi^I_{,3}\end{pmatrix}$	$F^T=\frac{1}{4\pi}R^I$	Unit flux $T=\frac{1}{4\pi k_0}\frac{1}{R^I}$	Both Galerkin vectors are in the same format, and direct result equivalence is proper.
Half-space, surface source	$\boldsymbol{F}=\frac{1}{8\pi(1-\nu)}\begin{bmatrix}0\\0\\\begin{bmatrix}R^I+(3-4\nu)R\\-4HD\theta\end{bmatrix}\end{bmatrix}^T$ from Ref. [65]	Unit force $4\pi Gu_z=\frac{2(1-\nu)}{R^I}+\frac{z^2}{R^{I3}}$	$F^T=\frac{1}{2\pi}R^I$	Unit flux $T=\frac{1}{2\pi k_0}\frac{1}{R^I}$ from Ref. [6]. This is the same as Eq. (12)	Two Galerkin vectors are in different formats, but direct result equivalence is proper.
Half-space, internal source	$\boldsymbol{F}=\frac{1}{8\pi(1-\nu)}\begin{bmatrix}0&0&\begin{bmatrix}R^I\\+(3-4\nu)R\\-2z\cdot z'\phi\\-4Dz'\psi\\-4HD\theta\end{bmatrix}\end{bmatrix}$ from Ref. [65]	Unit force $16\pi G(1-\nu)u_z=\frac{3-4\nu}{R^I}+\frac{(z-z')^2}{R^{I3}}+\frac{8(1-\nu)^2-(3-4\nu)}{R}+\frac{(3-4\nu)(z+z')^2-2z\cdot z'}{R^3}+\frac{6z\cdot z'(z+z')^2}{R^5}$	$F^T=\frac{1}{4\pi}(R^I+R)$	Unit flux $T=\frac{1}{4\pi k_0}\left(\frac{1}{R^I}+\frac{1}{R}\right)$ This work	The same as above
Full space, eigenstrains	$\boldsymbol{F}=\frac{G}{4\pi(1-\nu)}\int_\Omega(2\nu e_{kk}\boldsymbol{g}_c-e_{jk}\boldsymbol{g}_{jk})d\boldsymbol{x}'$ Details of $\boldsymbol{g_c}$ and $\boldsymbol{g_{kj}}$ in Ref. [63].	$-8\pi Hu_i=4H\int_\Omega e_{im}\phi^I_{,m}d\boldsymbol{x}'-\int_\Omega(e_{km}R^I_{,kmi}-2\nu e_{kk}\phi^I_{,i})d\boldsymbol{x}'$ from Ref. [63]	The integral core $\boldsymbol{f^T}=-\frac{k_0}{4\pi}\Delta T^*_j R^I_{,j}$	The integral core $T=-\frac{1}{4\pi}\Delta T^*_j\phi^I_{,j}$ from Refs. [55,64]	Two Galerkin vectors are in different formats, and direct result simplification not applicable due to the involvement of g_c, F_1, F_2 in the elastic displacement solution.
Half-space, eigenstrains	$\boldsymbol{F}=\frac{G}{4\pi(1-\nu)}\int_\Omega(2\nu e_{kk}\boldsymbol{g}_c-e_{jk}\boldsymbol{g}_{jk})d\boldsymbol{x}'$ Details of $\boldsymbol{g_c}$ and $\boldsymbol{g_{kj}}$ in Ref. [15,60].	$2Gu_i=2(1-\nu)F_{i,jj}-F_{j,ji}$ Details in Ref. [15]	The integral core $\boldsymbol{f^T}=-\frac{k_0}{4\pi}\Delta T^*_j(R^I_{,j}-R_{,j})$	The integral core $T=\frac{1}{4\pi}\Delta T^*_j(\phi^I_{,j}-\phi_{,j})$ from Ref. [64]	The same as above.

Consider a homogeneous and isotropic half-space, $\mathcal{B}$, subjected to static surface electrical flux $i_e(x, y)$ and surface magnetic flux $i_m(x, y)$. For any material point (x, y, z) inside $\mathcal{B}$, the boundary conditions are

$$D(x, y, 0, t) = -i_e(x, y, t) \tag{39}$$

$$B(x, y, 0, t) = -i_m(x, y, t) \tag{40}$$

The electromagnetic variables can make a complete analogy set with the thermal variables as illustrated in Fig. 1, i.e.

$$\begin{aligned}\text{electric potential } \varphi &\leftrightarrow \text{magnetic potential } \phi \\ &\leftrightarrow \text{temperature } T\end{aligned} \tag{41}$$

$$\text{electrical flux } i_e \leftrightarrow \text{magnetic flux } i_m \leftrightarrow \text{heat flux } \bar{q} \tag{42}$$

$$\text{permittivity } \varpi_0 \leftrightarrow \text{permeability } \mu_0 \leftrightarrow \text{conductivity } k_0 \tag{43}$$

$$\text{free charge density } \rho_f \leftrightarrow \text{heat source } q_0 \tag{44}$$

Likewise, this affects the equivalence between elasticity and static electromagnetics.

2.6 Analogy in MEMCT Field Coupling. The generalized constitutive equations can be written as follows to complement the MEMCT coupling theory [2]

$$\Psi = \mathbf{M} \cdot \Phi_{,i} \tag{45}$$

where the generalized dual variable collection is $\Psi = (\sigma_{ij} \leftrightarrow -q_i \leftrightarrow -D_i \leftrightarrow -B_i \leftrightarrow -\xi_i)$, the state variable collection is $\Phi_{,i} = (\varepsilon_{ij} \leftrightarrow -\theta_i \leftrightarrow -E_i \leftrightarrow -H_i \leftrightarrow -\vartheta_i)$, and the generalized material matrix, $[\mathbf{M}]$, includes the coupling properties is

$$\mathbf{M} = \begin{bmatrix} c_{ijkl} & \lambda_{ijk} & e_{ijk} & d_{ijk} & a_{ijk} \\ & k_{ij} & h_{ij} & m_{ij} & b_{ij} \\ & & \varpi_{ij} & g_{ij} & t_{ij} \\ & \text{sym.} & & \mu_{ij} & s_{ij} \\ & & & & \beta_{ij} \end{bmatrix} \tag{46}$$

The diagonal terms in $[\mathbf{M}]$ are the material properties, C, in each individual field, and $C_M = (c_{ijkl} \leftrightarrow k_{ij} \leftrightarrow \varpi_{ij} \leftrightarrow \mu_{ij} \leftrightarrow \beta_{ij})$, and the other elements in $[\mathbf{M}]$ denote the field coupling parameters, A, with $A = (\lambda_{ijk} \leftrightarrow e_{ijk} \leftrightarrow d_{ijk} \leftrightarrow a_{ijk} \leftrightarrow h_{ij} \leftrightarrow m_{ij} \leftrightarrow b_{ij} \leftrightarrow g_{ij} \leftrightarrow t_{ij} \leftrightarrow s_{ij})$. For example, λ_{ijk}, e_{ijk}, d_{ijk}, and a_{ijk} are the elastic-thermal tensor, piezoelectric tensor, piezomagnetic tensor, and elastic-chemical tensor, respectively, where $\lambda_{ij} = c_{ijkl}\alpha_{kl}$ with α_{kl} denoting thermal expansion coefficients. h_{ij}, m_{ij}, b_{ij}, g_{ij}, t_{ij}, and s_{ij} are the pyroelectric coefficient, pyroelectric coefficient, pyrochemical coefficient, magnetoelectric coefficient, electric-chemical constant, and magnetic-chemical constant, respectively. The detail definitions of material parameters are given in the Appendix of [2]. The analyses in Sec. 2.5 show that the lower-order variables can be obtained from degrading the corresponding higher-order mechanical variables and the equivalating related material properties. Besides the material properties C_M pertaining to each individual field, in the field coupling parameters $A = (\lambda_{ijk} \leftrightarrow e_{ijk} \leftrightarrow d_{ijk} \leftrightarrow a_{ijk} \leftrightarrow h_{ij} \leftrightarrow m_{ij} \leftrightarrow b_{ij} \leftrightarrow g_{ij} \leftrightarrow t_{ij} \leftrightarrow s_{ij})$, the mechanics-related coupling parameters, $\lambda_{ijk} \leftrightarrow e_{ijk} \leftrightarrow d_{ijk} \leftrightarrow a_{ijk}$, are also in higher orders. As an example, the thermo-electro-mechanical solutions for multilayered materials can be obtained from the recent multilayered electromagnetic-mechanical solutions [67] by using the equivalences of (i) dual variables $(q_i \leftrightarrow B_i)$, (ii) state variables $(\theta_i \leftrightarrow H_i)$, (iii) individual parameters $(k_{ij} \leftrightarrow \mu_{ij})$, and (iv) coupling parameters $(\lambda_{ijk} \leftrightarrow d_{ijk})$ and $(h_{ij} \leftrightarrow g_{ij})$, where h_{ij} are the pyroelectric coefficients and g_{ij} the magnetoelectric coefficients.

3 An Application Case

Material interfaces between two or more constituent solids with different properties are commonly found in various material structures, such as the coating-substrate interface in layered materials and inclusion-matrix interface in composites [68–70]. Due to property mismatching, crystal defects, or impurity diffusion, the material interfaces may involve a bonding issue. The imperfect interfaces would affect the transmissions of force and/or displacement in elasticity [69], influence heat transfer [71,72], cause the imperfect gluing and/or soldering in electronic packaging [71], and reduce the charge-diffusion rate in batteries [73]. The imperfect interfaces in elasticity have been addressed most deeply, such as the spring-like interface in layered materials [74], coupled dislocation-like and force-like interfaces in layered materials [69] and in joined half-spaces [70,75]. Figure 3 illustrates an example of a layered half-space with imperfect layer-substrate interfaces, where the layer thickness is h, and a uniform force, or heat flux, or electric/magnetic flux, or diffusion flux, is applied on the top surface of the layer. Note that Fig. 3 is for the steady-state conditions, while the scheme for transient conditions for convection diffusion can be referenced to the example by the lattice Boltzmann method [76].

As described in Ref. [74], set imperfect mechanical interface conditions, known as the spring-like conditions of layered materials, can be written as

$$\begin{aligned}&\kappa_c[u_i^L(x, y, h) - u_i^S(x, y, 0)] = -\sigma_{3i}^L(x, y, h) \\ &\sigma_{3i}^L(x, y, h) = \sigma_{3i}^S(x, y, 0) \\ &\kappa_c \in [0, \infty);\ i = 1, 2, 3\end{aligned} \tag{47}$$

where κ_c is a spring-imperfection index, superscript S or L is used to distinguish variables associated with the layer or the substrate half-space, and h denotes the layer thickness. The spring-like interface conditions in Eq. (47) show that the interfacial stresses are continuous, but the interfacial displacements are discontinuous, governed by the spring index κ_c. When κ_c is infinite, $u_i^L(x, y, h)$ approaches $u_i^S(x, y, 0)$, which is referred to as the perfectly bonded interface condition. A debonding interface occurs when κ_c approaches zero.

As described in Refs. [71,77], the imperfect thermal impedance conditions of the layered materials can be written as

$$\begin{aligned}&r_t[T^L(x, y, h) - T^S(x, y, 0)] = q_3^L(x, y, h) \\ &q_3^L(x, y, h) = q_3^S(x, y, 0) \\ &r_t \in [0, \infty)\end{aligned} \tag{48}$$

where r_t is the thermal conductance, and q_3 is the normal heat flux. When $r_t = 0$, the interface is a complete thermal barrier, while heat conduction across the interface is perfect as r_t approaches infinity.

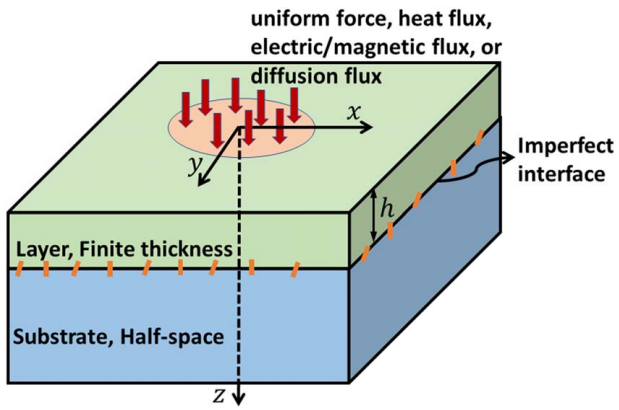

Fig. 3 Illustration of a layered half-space with imperfect interfaces, and a uniform force, heat flux, electric/magnetic flux, or diffusion flux, is applied on a region of the top surface of the layer

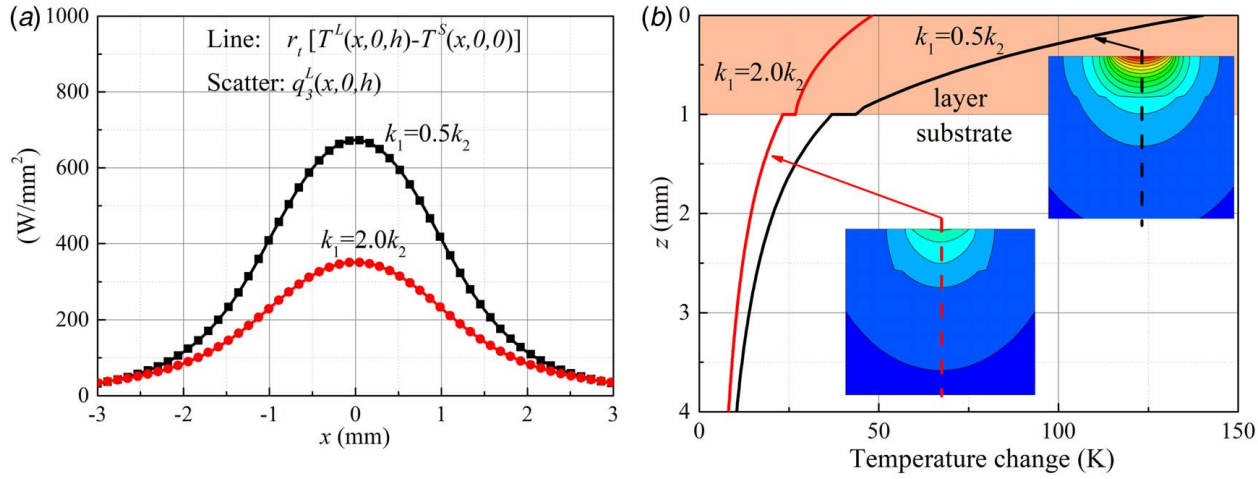

Fig. 4 (*a*) Interfacial heat flux and temperature difference and (*b*) subsurface temperature change, of a layered half-space material system with an imperfect thermal interface, solved with the current equivalence method via the elastic solutions, for the problem of a uniform surface heat input of density 2000 W/mm^2 on the region $\sqrt{x^2+y^2} \le 1.0$ mm. The substrate conductivity is $k_2 = 25$ W/mm · K, the layer conductivity is $k_1 = 0.5k_2$ or $2.0k_2$, the layer thickness is $h = 1.0$ mm, and the thermal conductance $r_t = 100$ W/mm^2 · K.

As mentioned in Refs. [78–80], the imperfect magnetoelectric interface conditions are given by

$$\begin{aligned} & r_e[\varphi^L(x,y,h) - \varphi^S(x,y,0)] = D_3^L(x,y,h) \\ & D_3^L(x,y,h) = D_3^S(x,y,0) \\ & r_e \in [0,\infty) \end{aligned} \tag{49}$$

and

$$\begin{aligned} & r_m[\phi^L(x,y,h) - \phi^S(x,y,0)] = B_3^L(x,y,h) \\ & B_3^L(x,y,h) = B_3^S(x,y,0) \\ & r_m \in [0,\infty) \end{aligned} \tag{50}$$

where r_e is the electric capacitor parameter, r_m is the magnetic inductor parameter, D_3 denotes the normal electric displacement, B_3 is the normal magnetic induction. When $r_e = 0$, the interface is a complete electric barrier, while the electric conduction across the interface is perfect as r_e approaches infinity. Likewise, when $r_m = 0$, the interface becomes a complete magnetic barrier, while the interface is magnetically perfect as r_m approaches infinity.

The mass diffusion imperfect interface conditions are given by [81,82]

$$\begin{aligned} & r_c[N^L(x,y,h) - N^S(x,y,0)] = \xi_3^L(x,y,h) \\ & \xi_3^L(x,y,h) = \xi_3^S(x,y,0) \\ & r_c \in [0,\infty) \end{aligned} \tag{51}$$

where r_c is the transmission parameter, N is the mass concentration, ξ_3 is the normal diffusion flux. Similarly, if $r_c = 0$, the interface is a complete diffusion barrier, while the solution transmission is perfect as r_c approaches infinity.

Based on the analogies of field collection $\Phi = (u_3 \leftrightarrow T \leftrightarrow \varphi \leftrightarrow \phi \leftrightarrow N)$, and dual variable collection $\Psi = (\sigma_{3j} \leftrightarrow -q_3 \leftrightarrow -D_3 \leftrightarrow -B_3 \leftrightarrow -\xi_3)$, the imperfect conditions in Eqs. (31)–(34) can be equivalent by letting $\kappa_c \leftrightarrow r_t \leftrightarrow r_e \leftrightarrow r_m \leftrightarrow r_c$, for the problem illustrated in Fig. 3. Figures 4 and 5 show the thermal and electric behaviors of this layered half-space with imperfect thermal and electric interfaces, respectively, solved by the current equivalence method based on the elastic solutions in Ref. [74] using the DC-FFT algorithm [59] with a 256 × 256 × 100 grid for the domain of 6.0 mm × 6.0 mm × 4.0 mm. The layer thickness is $h = 1.0$ mm. Figure 4(*a*) plots the interfacial heat flux $q_3^L(x,y,h)$, as well as the interfacial temperature difference, with thermal conductance $r_t = 100$ W/mm^2 · K, for the problem of a uniform surface heat input of density 2000 W/mm^2 on the region $\sqrt{x^2+y^2} \le 1.0$ mm. The substrate conductivity is $k_2 = 25$W/mm · K, and the layer conductivity is $k_1 = 0.5k_2$ or $2.0k_2$. The value of $r_t[T^L(x,y,h) - T^S(x,y,0)]$ well agrees with $q_3^L(x,y,h)$, which is identical to the imperfectly thermal boundary condition (Eq. (48)). Furthermore, Fig. 4(*b*) shows the subsurface temperature distributions along the z-direction for heat conductivities of $k_1 = 0.5k_2$ and $2.0k_2$. The temperature is discontinuous in the layer-substrate interface ($z = h = 1.0$ mm) due to the imperfect thermal boundary condition.

Figure 5(*a*) plots the interfacial electric flux $D_3^L(x,y,h)$, as well as the interfacial electric potential difference, solved by using the current equivalence method, with electric capacitor parameter $r_e = 1.5 \times 10^{-2}$ C^2/Nmm^3, for the problem of a uniform surface electric flux of density 2×10^{-2} C/mm^2 on region $\sqrt{x^2+y^2} \le 1.0$ mm. The substrate dielectric permittivity is $\varpi_2 = 1 \times 10^{-2}$ C^2/N · mm^2, and the layer permittivity is $\varpi_1 = 0.5\varpi_2$ or $2.0\varpi_2$. The value of $r_e[\varphi^L(x,y,h) - \varphi^S(x,y,0)]$ well agrees with $D_3^L(x,y,h)$, which is identical to the imperfect electric boundary condition given in Eq. (32). Figure 5(*b*) shows the subsurface electric potential distributions along the z-direction for dielectric permittivities of $\varpi_1 = 0.5\varpi_2$ and $2.0\varpi_2$. The electric potential is discontinuous in the layer-substrate interface ($z = h = 1.0$ mm) due to the imperfect electric boundary condition. The distribution behaviors of temperature T and electric potential φ are similar, so are magnetic potential ϕ and mass concentration N, all obeying the analogies of field collection $\Phi = (u_3 \leftrightarrow T \leftrightarrow \varphi \leftrightarrow \phi \leftrightarrow N)$.

4. Discussion and a Concept of Multifield Sensing

4.1 Concept Description. As shown in Sec. 2, a systematic analogy and unified computation methodology from elasticity to electromagnetic-chemical-thermal fields are developed by setting Poisson's ratio $\nu \to 0.5$ and removing terms multiplied by z with power n. It leads to the identical surface-value relation of the elastic and thermal (or chemical, electric, magnetic) fields if the material is incompressible ($\nu = 0.5$) because the z^n-multiplied terms automatically disappear at $z = 0$. These existing surface-value equivalences indicate that if the surface elastic field of an incompressible material is measured under a unit surface force, the surface thermal (or chemical, electric, magnetic) field under a unit specific flux can be immediately obtained by using parameter conversion without additional thermal (or chemical, electric, magnetic)

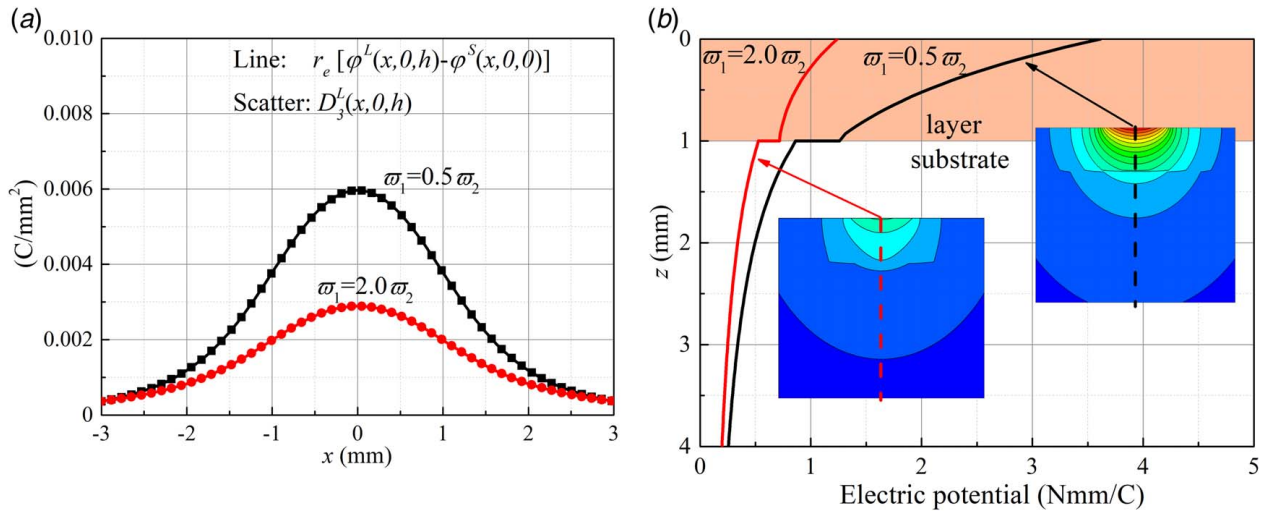

Fig. 5 (*a*) Interfacial electric flux and electric potential difference and (*b*) subsurface electric potential, of a layered half-space material system with an imperfect electric interface, solved by the current equivalence method *via* the elastic solutions, for the problem of a uniform surface electric flux of density 2×10^{-2} C/mm^2 on the region $\sqrt{x^2+y^2}\le 1.0$ mm. The substrate dielectric permittivity is $\varpi_2=1\times10^{-2}$ C^2/N · mm^2, the layer permittivity is $\varpi_1=0.5\varpi_2$ or $2.0\varpi_2$, the layer thickness is $h=1.0$ mm, and the electric capacitor parameter $r_e=1.5\times10^{-2}$ C^2/Nmm^3.

measurement. For example, the surface-value equivalence for displacement and temperature at any meaningful surface location is $u_{z0}(v\to 0.5)=\frac{k_0T_0}{2G}$, caused by unit surface point fluxes, where $u_{z0}=u_z(x,y,z=0)$ and $T_0=T(x,y,z=0)$.

For practical materials which is not incompressible, the following relationship can be obtained from Eq. (11)

$$\frac{u_{z0}}{u_{z0}(v\to 0.5)}=2(1-\nu) \tag{52}$$

Equation (52) indicates that the equivalence from surface elasticity to the thermal (or chemical, electric, magnetic) field can be achieved by dividing $2(1-\nu)$, which leads to the following

$$\begin{aligned}&\beta_0N_0\leftrightarrow\varpi_0\varphi_0\leftrightarrow\mu_0\phi_0\leftrightarrow k_0T_0\\&\leftrightarrow 2Gu_{z0}(v\to 0.5)=\frac{G}{(1-\nu)}u_{z0}\end{aligned} \tag{53}$$

where N_0 is the surface mass concentration, φ_0 is the surface electric potential, ϕ_0 is the surface magnetic potential, and T_0 is the surface potential. Equation (53) manifests that if the surface elastic field of a material is measured under a unit force, the surface thermal (or chemical, electric, magnetic) field under a unit-specific flux can be immediately obtained through dividing the elastic response by $2(1-\nu)$.

In fact, if one of these surface field values can be measured under a certain flux strength, the other four under the same shapes of flux distributions can be immediately obtained through Eq. (53). This means that a multifield-multifunctional sensor can be built with one measurement system. Further, with the boundary values known, the entire distribution of one field can be conveniently predicted by the corresponding model. This suggests a multifield model-based monitoring system supported with the multifield-multifunctional surface sensor.

4.2 Case of Using a Thermal Couple for Displacement Measurement. The concept of multifield sensing can be implemented to measure the surface elastic field via temperature monitoring, or sense the thermal field via surface normal displacement monitoring at one location, or certain locations, by means of the analogy methodology and the surface-value equivalence approach presented in Sec. 4.1. Consider the upper body shown by the left plot of Fig. 6, which is under a steady sliding, or its mating surface is sliding; it receives a steady-state surface heat flux due to friction. The surface radius of this body is R, loaded by surface pressure and heat flux of distribution radius r. The normal displacement or temperature sensors can be located anywhere at the surface from 0 to $10r$ from the centerline of the body and $r<R/10$ to satisfy the half-space assumption.

If the Coulomb friction is considered, the frictional heat flux and pressure are in the same shapes of distributions but proportional in values, i.e.,

$$\textit{Heat flux}=\textit{heat coefficient}\times\textit{pressure}=\mu_T\times\textit{pressure} \tag{54}$$

where *heat coefficient* μ_T equals to friction coefficient × velocity × heat partition coefficient.

When the thermal couple at location X measures surface temperature $T_0(X)$, surface normal displacement $u_{z0}(X)$ is immediately obtained based on the equivalence equation Eq. (53) without using a displacement sensor. The calculation expression is

$$u_{z0}(X)=\frac{(1-\nu)k_0T_0(X)}{G\mu_T} \tag{55}$$

Again, μ_T is the *heat coefficient* in Eq. (54), k_0 is the heat conductivity, G is the shear modulus, ν is the Poisson's ratio. Note that convolution calculation should have been involved; however, the same shape of pressure and frictional heating distributions cancels the convolution operation. Note here, shear traction induced normal displacement is not included.

Equation (55) shows another exciting result; no matter the surface sources are concentrated or distributed, mechanical or others, the relationship of the responses at X still obeys that for concentrated sources as long as the corresponding distribution shapes are the same. This offers a great convenience for sensing, and one sensor, one calculation, applies to all types of loading with simple parameter conversions. The equivalence equations for other fields are given as follows:

$$\begin{aligned}u_{z0}(X)&=\frac{(1-\nu)k_0T_0(X)}{G\mu_T}=\frac{(1-\nu)\varpi_0\varphi_0(X)}{G\mu_E}=\frac{(1-\nu)\mu_0\phi_0(X)}{G\mu_M}\\&=\frac{(1-\nu)\beta_0N_0(X)}{G\mu_D}\end{aligned} \tag{56}$$

where μ_T, μ_E, μ_M, and μ_D are the heat coefficient, electric-

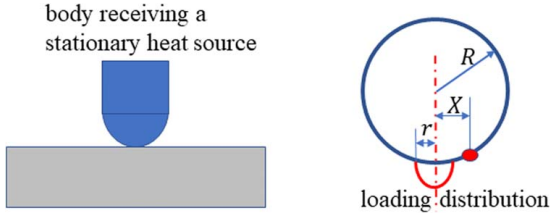

Fig. 6 Sensing the displacement and temperature fields of a body under steady sliding

mechanical ratio, magnetic-mechanical ratio, and diffusion-mechanical ratio, respectively. Those coefficients evaluate the proportional values between the flux and pressure, along with their same shapes of distributions, as discussed below Eq. (53) and above Eq. (54). If these coefficients and ratios are set to unit, Eq. (56) becomes Eq. (53).

However, caution should be given to material property variations. The rate of degradation of the material parameters pertaining to one field may be different from that of the parameters of another field. In-depth material studies are needed.

5 Conclusions

A systematic analogy and unified computation methodology from elasticity to electromagnetic-chemical-thermal fields have been developed based on the similarities of mechanical-electromagnetic-chemical-thermal (MEMCT) field variables, governing equations, and the material properties pertaining to each individual field. For an homogeneous material, or layered material set, subjected to different surface flux, the thermal, electromagnetic, or chemical solutions can be obtained from the direct degeneration of the corresponding elastic solutions in the same way, instead of solving individual problems in each field, by making

(1) Poisson's ratio $\nu \to 0.5$;
(2) equivalences of $2G \leftrightarrow k_0 \leftrightarrow \varpi_0 \leftrightarrow \mu_0 \leftrightarrow \beta_0$ with G for shear modulus, k_0 for heat conductivity, ϖ_0 for dielectric permittivity, μ_0 for magnetic permeability, and β_0 for chemical diffusivity;
(3) removal of the terms that involve z (and its equivalent, h), or z^n, as a multiplier in elastic solutions if excited along the z-direction; and likewise, removal of terms with $x-$ or $y-$ multiplication if the excitation source is along the x- or y-direction;
(4) equivalences of $\omega_e^2 \leftrightarrow -\frac{\mathrm{i}C_p}{2}\omega_t \leftrightarrow -\frac{\mathrm{i}}{2}\omega_c$, with ω_e for elastic wave frequency, ω_t for thermal wave frequency, and ω_c for diffusion frequency. These equivalences also mark the time-scale differences in different fields.

For static fields, or steady-state elastic, thermal, and chemical fields, measuring one at the surface excited by one type flux is sufficient to sense the others at the same location due to their corresponding flux, and thus a multifunctional sensing system can be developed using one sensor. Furthermore, no matter the surface sources are concentrated or distributed, mechanical or others, the relationship of the responses at the same surface location obeys that for concentrated sources if the corresponding distribution shapes are the same.

The thermal, electromagnetic, and chemical responses of a layered half-space material system with imperfect thermal, electromagnetic, or chemical interfaces have been explored, and the results further confirm that the solutions can be directly obtained by applying the proposed analogy methodology to the elastic solutions.

However, for inhomogeneous materials, the analogy should be done at the stage of the fundamental solutions, for example, the Galerkin-vector stage.

Acknowledgment

The authors would like to thank the support of the Center for Surface Engineering and Tribology at Northwestern University, USA. Zhang X. would also like to acknowledge the supports by the National Natural Science Foundation of China (12102085), the Postdoctoral Science Foundation of China (2020M683278, 2021T140091), and the Sichuan Science and Technology Program (2021YFG0217).

Conflict of Interest

There are no conflicts of interest. This article does not include research in which human participants were involved. This article does not include any research in which animal participants were involved.

Data Availability Statement

The datasets generated and supporting the findings of this article are obtainable from the corresponding author upon reasonable request. The authors attest that all data for this study are included in the paper.

References

[1] Dincer, I., and Cengel, Y., 2001, "Energy, Entropy and Exergy Concepts and Their Roles in Thermal Engineering," Entropy, **3**(3), pp. 116–149.
[2] Zhang, X., Wang, Q. J., and Shen, H., 2018, "A Multi-Field Coupled Mechanical-Electric-Magnetic-Chemical-Thermal (MEMCT) Theory for Material Systems," Comput. Methods Appl. Mech. Eng., **341**, pp. 133–162.
[3] Zhang, X., Wang, Q. J., Harrison, K. L., Jungjohann, K., Boyce, B. L., Roberts, S. A., Attia, P. M., and Harris, S. J., 2019, "Rethinking How External Pressure Can Suppress Dendrites in Lithium Metal Batteries," J. Electrochem. Soc., **166**(15), pp. A3639–A3652.
[4] Zhang, X., Wang, Q. J., Harrison, K. L., Roberts, S. A., and Harris, S. J., 2020, "Pressure-Driven Interface Evolution in Solid-State Lithium Metal Batteries," Cell Rep Phys. Sci., **1**(2), p. 100012.
[5] Timoshenko, S. P., and Gere, J. M., 2009, *Theory of Elastic Stability*, Dover Publications, New York.
[6] Johnson, K. L., 1987, *Contact Mechanics*, Cambridge University Press, Cambridge, UK.
[7] Huajian, G., Cheng-Hsin, C., and Jin, L., 1992, "Elastic Contact Versus Indentation Modeling of Multi-Layered Materials," Int. J. Solids Struct., **29**(20), pp. 2471–2492.
[8] Yu, C., Wang, Z., and Wang, Q. J., 2014, "Analytical Frequency Response Functions for Contact of Multilayered Materials," Mech. Mater., **76**, pp. 102–120.
[9] Zhang, X., Wang, Q. J., and He, T., 2020, "Transient and Steady-State Viscoelastic Contact Responses of Layer-Substrate Systems With Interfacial Imperfections," J. Mech. Phys. Solids, **145**, p. 104170.
[10] Suresh, S., 2001, "Graded Materials for Resistance to Contact Deformation and Damage," Science, **292**(5526), pp. 2447–2451.
[11] Zhang, X., Wang, Q. J., Wang, Y., Wang, Z., Shen, H., and Liu, J., 2018, "Contact Involving a Functionally Graded Elastic Thin Film and Considering Surface Effects," Int. J. Solids Struct., **150**, pp. 184–196.
[12] Eshelby, J. D., 1957, "The Determination of the Elastic Field of an Ellipsoidal Inclusion, and Related Problems," Proc. R. Soc. London, A, **241**(1226), pp. 376–396.
[13] Mori, T., and Tanaka, K., 1973, "Average Stress in Matrix and Average Elastic Energy of Materials With Misfitting Inclusions," Acta Metall., **21**(5), pp. 571–574.
[14] Hill, R., 1963, "Elastic Properties of Reinforced Solids: Some Theoretical Principles," J. Mech. Phys. Solids, **11**(5), pp. 357–372.
[15] Liu, S., Jin, X., Wang, Z., Keer, L. M., and Wang, Q., 2012, "Analytical Solution for Elastic Fields Caused by Eigenstrains in a Half-Space and Numerical Implementation Based on FFT," Int. J. Plast., **35**, pp. 135–154.
[16] Gao, H., Huang, Y., Nix, W., and Hutchinson, J., 1999, "Mechanism-Based Strain Gradient Plasticity—I. Theory," J. Mech. Phys. Solids, **47**(6), pp. 1239–1263.
[17] Huang, Y., Gao, H., Nix, W., and Hutchinson, J., 2000, "Mechanism-Based Strain Gradient Plasticity—II. Analysis," J. Mech. Phys. Solids, **48**(1), pp. 99–128.
[18] Yang, F., Chong, A., Lam, D. C. C., and Tong, P., 2002, "Couple Stress Based Strain Gradient Theory for Elasticity," Int. J. Solids Struct., **39**(10), pp. 2731–2743.
[19] Toupin, R. A., 1964, "Theories of Elasticity With Couple-Stress," Arch. Ration. Mech. Anal., **17**(2), pp. 85–112.
[20] Mindlin, R., 1963, "Influence of Couple-Stresses on Stress Concentrations," Exp. Mech., **3**(1), pp. 1–7.
[21] Wang, Y., Shen, H., Zhang, X., Zhang, B., Liu, J., and Li, X., 2018, "Semi-Analytical Study of Microscopic Two-Dimensional Partial Slip Contact

Problem Within the Framework of Couple Stress Elasticity: Cylindrical Indenter," Int. J. Solids Struct., **138**, pp. 76–86.
[22] Carslaw, H. S., and Jaeger, J. C., 1959, *Conduction of Heat in Solids*, Clarendon Press, Oxford.
[23] Tadeu, A., and Simões, N., 2006, "Three-Dimensional Fundamental Solutions for Transient Heat Transfer by Conduction in an Unbounded Medium, Half-Space, Slab and Layered Media," Eng. Anal. Boundary Elem., **30**(5), pp. 338–349.
[24] Reitzle, D., Geiger, S., and Kienle, A., 2019, "Semi-Analytical Solution of the Time-Dependent Heat Equation for Three-Dimensional Anisotropic Multi-Layered Media," Int. J. Heat Mass Transfer, **134**, pp. 984–992.
[25] Zhang, X., He, T., Miwa, H., Nanbu, T., Murakami, R., Liu, S., Cao, J., and Wang, Q. J., 2019, "A New Approach for Analyzing the Temperature Rise and Heat Partition at the Interface of Coated Tool Tip-Sheet Incremental Forming Systems," Int. J. Heat Mass Transfer, **129**, pp. 1172–1183.
[26] Zhang, H., Liu, S., Han, S., and Fan, L., 2019, "The Numerical Manifold Method for Crack Modeling of Two-Dimensional Functionally Graded Materials Under Thermal Shocks," Eng. Fract. Mech., **208**, pp. 90–106.
[27] Xi, Q., Fu, Z.-J., and Rabczuk, T., 2019, "An Efficient Boundary Collocation Scheme for Transient Thermal Analysis in Large-Size-Ratio Functionally Graded Materials Under Heat Source Load," Comput. Mech., **64**(5), pp. 1221–1235.
[28] Yang, W., Zhou, Q., Huang, Y., Wang, J., Jin, X., and Keer, L. M., 2019, "A Thermoelastic Contact Model Between a Sliding Ball and a Stationary Half Space Distributed With Spherical Inhomogeneities," Tribol. Int., **131**, pp. 33–44.
[29] Shi, X., Wang, L., Zhou, Q., and Wang, Q., 2018, "A Fast Approximate Method for Heat Conduction in an Inhomogeneous Half-Space Subjected to Frictional Heating," ASME J. Tribol., **140**(4), p. 041101.
[30] Liu, J., Xu, S., and Zeng, Q., 2017, "A Multi-Scale Micromechanical Investigation on Thermal Conductivity of Cement-Based Composites," IOP Conf. Ser.: Mater. Sci. Eng., **167**, p. 012069.
[31] Maxwell, J. C., 1873, *A Treatise on Electricity and Magnetism*, Clarendon Press, Oxford.
[32] Stratton, J. A., 2007, *Electromagnetic Theory*, John Wiley & Sons, New York.
[33] Adkins, J., 1963, "Non-Linear Diffusion-Non-Linear Diffusion II. Constitutive Equations for Mixtures of Isotropic Fluids," Philos. Trans. R. Soc. London, Ser. A, **255**(1064), pp. 635–650.
[34] Green, A. E., and Naghdi, P. M., 1965, "A Dynamical Theory of Interacting Continua," Int. J. Eng. Sci., **3**(2), pp. 231–241.
[35] Bowen, R., 1967, "Toward a Thermodynamics and Mechanics of Mixtures," Arch. Ration. Mech. Anal., **24**(5), pp. 370–403.
[36] Rajagopal, K., and Tao, L., 1995, *Mechanics of Mixtures*, World Scientific, Singapore.
[37] Zhang, X., Wang, Q. J., Zeng, Z., Wu, Y., and Peng, B., 2021, "An LT-FFT Based Model for Diffusion-Affected Contacts," Tribol. Int., **157**, p. 106890.
[38] Cao, T. Y., 2019, *Conceptual Development of 20th Century Field Theories*, Cambridge University Press, Cambridge, UK.
[39] Zhao, Y., 2012, *Physical Mechanics of Surfaces and Interfaces (in Chinese)*, Beijing Science Press, Beijing, China.
[40] Zhao, Y., 2014, *Nano and Mesoscopic Mechanics (in Chinese)*, Beijing Science Press, Beijing, China.
[41] Einstein, A., and Infeld, L., 1971, *The Evolution of Physics*, Cambridge University Press, Cambridge, UK.
[42] Wise, M. N., 1979, "William Thomson's Mathematical Route to Energy Conservation: A Case Study of the Role of Mathematics in Concept Formation," Hist. Stud. Phys. Sci., **10**, pp. 49–83.
[43] Zhang, H., Liu, S., and Han, S., 2018, "The Numerical Manifold Method for Transient Moisture Diffusion in 2D Functionally Graded Materials," IOP Conf. Ser. Earth Environ. Sci., **189**, p. 032017.
[44] Jin, X., Wang, Z., Zhou, Q., Keer, L. M., and Wang, Q., 2014, "On the Solution of an Elliptical Inhomogeneity in Plane Elasticity by the Equivalent Inclusion Method," J. Elast., **114**(1), pp. 1–18.
[45] Chandrasekharaiah, D., and Cowin, S., 1989, "Unified Complete Solutions for the Theories of Thermoelasticity and Poroelasticity," J. Elast., **21**(1), pp. 121–126.
[46] Norris, A., 1992, "On the Correspondence Between Poroelasticity and Thermoelasticity," J. Appl. Phys., **71**(3), pp. 1138–1141.
[47] Faghri, A., Zhang, Y., and Howell, J. R., 2010, *Advanced Heat and Mass Transfer*, Global Digital Press, Columbia.
[48] Griffith, A. A., and Taylor, G. I., 1917, "The Use of Soap Films in Solving Torsion Problems," Proc. Inst. Mech. Eng., **93**(1), pp. 755–809.
[49] Benveniste, Y., and Milton, G., 2003, "New Exact Results for the Effective Electric, Elastic, Piezoelectric and Other Properties of Composite Ellipsoid Assemblages," J. Mech. Phys. Solids, **51**(10), pp. 1773–1813.
[50] Boulanger, P., and Hayes, M., 2003, "An Anisotropic Electromagnetic-Elastic Analogy," J. Appl. Math. Inf., **8**, pp. 17–33.
[51] Ikelle, L. T., 2012, "On Elastic-Electromagnetic Mathematical Equivalences," Geophys. J. Int., **189**(3), pp. 1771–1780.
[52] Thomson, B. K., and Thomson, W., 2010, *Baltimore Lectures on Molecular Dynamics and the Wave Theory of Light*, Cambridge University Press, Cambridge, UK.
[53] Hiroshi, H., and Minoru, T., 1986, "Equivalent Inclusion Method for Steady State Heat Conduction in Composites," Int. J. Eng. Sci., **24**(7), pp. 1159–1172.
[54] Hatta, H., and Taya, M., 1985, "Effective Thermal Conductivity of a Misoriented Short Fiber Composite," J. Appl. Phys., **58**(7), pp. 2478–2486.
[55] Hatta, H., and Taya, M., 1986, "Thermal Conductivity of Coated Filler Composites," J. Appl. Phys., **59**(6), pp. 1851–1860.
[56] Yang, W., Zhou, Q., Zhai, Y., Lyu, D., Huang, Y., Wang, J., Jin, X., Keer, L. M., and Wang, Q. J., 2019, "Semi-Analytical Solution for Steady State Heat Conduction in a Heterogeneous Half Space With Embedded Cuboidal Inhomogeneity," Int. J. Therm. Sci., **139**, pp. 326–338.
[57] Liu, S., Lannou, S., Wang, Q., and Keer, L., 2004, "Solutions for Temperature Rise in Stationary/Moving Bodies Caused by Surface Heating With Surface Convection," ASME J. Heat Transfer-Trans. ASME, **126**(5), pp. 776–785.
[58] Liu, S., and Wang, Q., 2002, "Studying Contact Stress Fields Caused by Surface Tractions With a Discrete Convolution and Fast Fourier Transform Algorithm," ASME J. Tribol., **124**(1), pp. 36–45.
[59] Liu, S., Wang, Q., and Liu, G., 2000, "A Versatile Method of Discrete Convolution and FFT (DC-FFT) for Contact Analyses," Wear, **243**(1–2), pp. 101–111.
[60] Yu, H., and Sanday, S., 1991, "Elastic Field in Joined Semi-Infinite Solids With an Inclusion," Proc. R. Soc. London, A, **434**(1892), pp. 521–530.
[61] Mindlin, R. D., 1936, "Force at a Point in the Interior of a Semi-Infinite Solid," Journal of Physics, **7**(5), pp. 195–202.
[62] Yu, H., and Sanday, S., 1990, "Axisymmetric Inclusion in a Half Space," ASME J. Appl. Mech., **57**(1), pp. 74–77.
[63] Liu, S., and Wang, Q., 2005, "Elastic Fields Due to Eigenstrains in a Half-Space," ASME J. Appl. Mech., **72**(6), pp. 871–878.
[64] Shi, X., Wang, Q., and Wang, L. J., 2019, "New Galerkin-Vector Theory and Efficient Numerical Method for Analyzing Steady-State Heat Conduction in Inhomogeneous Bodies Subjected to a Surface Heat Flux," Appl. Therm. Eng., **161**, p. 113838.
[65] Mindlin, R. D., and Cheng, D. H., 1950, "Nuclei of Strain in the Semiic Fields Caused," J. Appl. Phys., **21**(9), pp. 926–930.
[66] Zhang, X., Wang, Z., Shen, H., and Wang, Q. J., 2018, "Dynamic Contact in Multiferroic Energy Conversion," Int. J. Solids Struct., **143**, pp. 84–102.
[67] Zhang, H., Wang, W., Liu, Y., and Zhao, Z., 2019, "Semi-Analytic Modelling of Transversely Isotropic Magneto-Electro-Elastic Materials Under Frictional Sliding Contact," Appl. Math. Model., **75**, pp. 116–140.
[68] Finnis, M. W., 1996, "The Theory of Metal-Ceramic Interfaces," J. Phys.: Condens. Matter, **8**(32), pp. 5811–5836.
[69] Wang, Z., Yu, H., and Wang, Q., 2017, "Layer-Substrate System With an Imperfectly Bonded Interface: Coupled Dislocation-Like and Force-Like Conditions," Int. J. Solids Struct., **122**, pp. 91–109.
[70] Li, D., Wang, Z., Yu, H., and Wang, Q., 2018, "Elastic Fields Caused by Eigenstrains in Two Joined Half-Spaces With an Interface of Coupled Imperfections: Dislocation-Like and Force-Like Conditions," Int. J. Eng. Sci., **126**, pp. 22–52.
[71] Vermeersch, B., and De Mey, G., 2007, "Influence of Thermal Contact Resistance on Thermal Impedance of Microelectronic Structures," Microelectron. Reliab., **47**(8), pp. 1233–1238.
[72] Antonetti, V., 1988, *Thermal Contact Resistance in Electronic Equipment, Heat Transfer in Electronic and Microelectronic Equipment*, Hemisphere Publishing Corporation, New York.
[73] Mizusaki, J., Saito, T., and Tagawa, H., 1996, "A Chemical Diffusion-Controlled Electrode Reaction at the Compact La_{1-x} Sr_xMnO_3/Stabilized Zirconia Interface in Oxygen Atmospheres," J. Electrochem. Soc., **143**(10), pp. 3065–3073.
[74] Wang, Z., Yu, H., and Wang, Q., 2017, "Layer-Substrate System With an Imperfectly Bonded Interface: Spring-Like Condition," Int. J. Mech. Sci., **134**, pp. 315–335.
[75] Li, D., Wang, Z., and Wang, Q., 2019, "Explicit Analytical Solutions for Elastic Fields in Two Imperfectly Bonded Half-Spaces With a Thermal Inclusion," Int. J. Eng. Sci., **135**, pp. 1–16.
[76] Yoshida, H., Kobayashi, T., Hayashi, H., Kinjo, T., Washizu, H., and Fukuzawa, K., 2014, "Boundary Condition at a Two-Phase Interface in the Lattice Boltzmann Method for the Convection-Diffusion Equation," Phys. Rev. E, **90**(1), p. 013303.
[77] Yovanovich, M. M., 2005, "Four Decades of Research on Thermal Contact, Gap, and Joint Resistance in Microelectronics," IEEE Trans. Compon. Packag. Technol., **28**(2), pp. 182–206.
[78] Fan, H., Yang, J., and Xu, L., 2006, "Piezoelectric Waves Near an Imperfectly Bonded Interface Between Two Half-Spaces," Appl. Phys. Lett., **88**(20), p. 203509.
[79] Otero, J., Rodríguez-Ramos, R., Bravo-Castillero, J., and Monsivais, G., 2012, "Interfacial Waves Between Two Piezoelectric Half-Spaces With Electro-Mechanical Imperfect Interface," Philos. Mag. Lett., **92**(10), pp. 534–540.
[80] Otero, J., Rodríguez-Ramos, R., Monsivais, G., Stern, C., Martínez, R., and Dario, R., 2014, "Interfacial Waves Between Two Magneto-Electro-Elastic Half-Spaces With Magneto-Electro-Mechanical Imperfect Interface," Philos. Mag. Lett., **94**(10), pp. 629–638.
[81] Angot, P., 2003, "A Model of Fracture for Elliptic Problems With Flux and Solution Jumps," C.R. Math., **337**(6), pp. 425–430.
[82] Angot, P., 1999, "Finite Volume Methods for Non Smooth of Diffusion Models: Application to Imperfect Contact Problems," Recent Advances in Numerical Methods and Applications II Proceeding of the Fourth International Conference, World Scientific, Singapore, pp. 621–629.